Journal of Advances in Medicine and Medical Research

34(2): 68-80, 2022; Article no.JAMMR.81351
ISSN: 2456-8899
(Past name: British Journal of Medicine and Medical Research, Past ISSN: 2231-0614, NLM ID: 101570965)

The Possible Role of Nanocurcumin in Rat Model of Statin Induced Myopathy: Histological and Immune Histochemical Study

Doha S. Mohamed [a], Nesreen G. Abdelhaleem [a], Ebtsam A. Shaaban [a*] and Ahmed M. Abu-Dief [b,c]

[a] Department of Histology, Faculty of Medicine, Sohag University, Sohag, Egypt.
[b] Department of Chemistry, Faculty of Science, Sohag University, Sohag-82534, Egypt.
[c] Department of Chemistry, College of Science, Taibah University, Madinah, P.O.Box 344, Saudi Arabia.

Authors' contributions

This work was carried out in collaboration among all authors. All authors read and approved the final manuscript.

Article Information

DOI: 10.9734/JAMMR/2022/v34i231263

Open Peer Review History:
This journal follows the Advanced Open Peer Review policy. Identity of the Reviewers, Editor(s) and additional Reviewers, peer review comments, different versions of the manuscript, comments of the editors, etc are available here: https://www.sdiarticle5.com/review-history/81351

Original Research Article

Received 06 December 2021
Accepted 11 February 2022
Published 23 February 2022

ABSTRACT

Background: Statins are the most commonly used drugs for reducing hypercholesterolemia. Unfortunately, statins induced myopathy is a common side effect of statins. Usually represented by fatigue, muscle pain, muscle tenderness, muscle weakness and nocturnal cramping. Curcumin has been proved as anti –inflammatory agent in the inflammatory conditions.
Aim: This research aimed to study the protective effect of nanocurcumin on the histological changes produced by atorvastatin in the skeletal muscles.
Material and Methods: A thirty albino rats (2-3 months old) were used in the present study.
The rats were randomly divided into four groups.
Group I: (five rats) and was used as a control group (control) , they were given 2 ml carboxy methyl cellulous (0.5%)orally through orogastric tube daily for 4 weeks.
Group II: (five rats) They were given nanocurcumin in a dose of 15ml \kg b.w orally through orogastric tube daily for 4weeks.
Group III: (ten rats) They were be given atorvastatin in a dose of 40 ml \kg b.w orally through orogastric tube daily for 4 weeks and divided into two subgroups.

**Corresponding author: E-mail: ebtesam.abdelrehem@med.sohag.edu.eg;*

Group III a (animal model): scarified 24h after the last dose.
Group III b (recovery group): scarified 2weeks after the last dose.
Group IV: (ten rats) they were given atorvastatin in a dose of 40 ml \kg b.w orally through orogastric for 4 weeks followed by nanocurcumin in a dose of 15mg \kg b.w orally daily for 4weeks.
Results: Degenerative and apoptotic changes were observed in the skeletal muscles in the atorvastatin treated groups, these changes could be attenuated by administration of nanocurcumin.
Conclusion: Apoptosis is a mechanism of atorvastatin induced myopathy. Nanocurcumin particles could attenuate this process and attenuated the toxicity of the drug. After stoppage of atorvastatin some of histopathological changes could be recovered.

Keywords: Statins; myopathy; curcumin; myositis; rhabdomyolysis.

1. INTRODUCTION

Myopathy is a weakness of skeletal muscles accompanied by tenderness, pain and elevation of the plasma creatinine kinase may be present. There are many different types of myopathies, some of which are genetic, inflammatory, or drug induced such as statin, Steroids or Zidovudine [1].

Statins are the most commonly used drugs for reducing hypercholesterolemia [2]. Myositis and/or rhabdomyolysis may occur in approximately 0.1% of statin-treated patients. [3].

Curcumin has proved it's benefit as anti-inflammatory agent in the inflammatory conditions [4], metabolic syndrome [5], pain [6] as well as in relieving inflammatory and degenerative eye conditions [7]. Unfortunately, the major problem associated with curcumin ingestion by itself, is it's poor bioavailability [8].

Nanoparticles of curcumin (nanocurcumin) were prepared by special chemical technique and were found to have a narrow particle size distribution in the range of 2-40 nm. Unlike curcumin, nanocurcumin was found to be freely dispersible in water in the absence of any surfactants.

The chemical structure of nanocurcumin was the same as that of curcumin, and there was no modification during nanoparticle preparation. Nano formulations of curcumin greatly transformed the way of treating diseases by improving its bio-availability, cellular uptake, and permeability with enhanced plasma concentration. Curcumin nanoparticles efficaciously distribute the exact therapeutic concentration of drug at the site of injury [9].

Numerous studies have been reported on the therapeutic efficacy of curcumin nanoformulations and explored its consequential properties against the wide range of human diseases [9].

This work aims to study the possible therapeutic effect of nanocurcumin on experimental statin induced myopathy.

2. MATERIALS

2.1 Chemicals

Atorvastatin was obtained from (Sigma Chemical Company, St. Louis, MO, USA). It was dissolved in carboxy methylcellulose before usage (0.5%). Curcumin (purity≥99%)was obtained from (Sigma Chemical Company, St. Louis, MO, USA) Nano curcumin was prepared at Chemistry department, Faculty of Sciences, Sohag University .

2.2 Preparation of Nanocurcumin

Curcumin (100 mg, 0.27 mmol) was dissolved in dichloromethane (20 mL). 1 mL of this solution was sprayed into boiling water (50 mL) dropwise with a flow rate of 0.2 mL/min in 5 minutes under ultrasonic conditions with an ultrasonic power of 100W and a frequency of 30 KHz. The contents were sonicated for 10 minutes and then stirred at room temperature for about 20 minutes when a clear orange colored solution was obtained. The solution was concentrated under reduced pressure at 50^{O} C and finally freeze dried to obtain an orange powder.

2.3 Particle Size Analysis

The mean particle diameter of curcumin nanoparticles was measured by transmission Electron Microscope (TEM). Analysis was done on a Morgagni 268 D from FEI (electron microscopy unit, Assuit university). The sample was prepared by placing a drop of the aqueous

dispersion of curcumin nanoparticles on the copper grid and allowing it to air dry.

Particle size distribution for the prepared nano curcumin was evaluated using image J Launcher, broken-symmetry software, version (1.4.3.6.7) [10,11,12].

2.4 Animals and Experimental Design

A thirty albino rats (2-3 months old) were used in the present study. Their weights ranged from 200-250 grams. The rats were maintained in a randomized 22^0c in a well-ventilated animal house in the Faculty of Medicine, Sohag University under natural photoperiod conditions and had free access to food and water during the course of the experiment.

The rats were randomized divided into four groups.

Group I : It includes five rats and was used as a control group (control) , they were given 2 ml carboxy methyl cellulous (0.5%)orally through orogastric tube daily for 4 weeks.

Group II: It includes five rats. They were given nanocurcumin in a dose of 15ml\kg b.w orally through orogastric tube daily for 4weeks.

Group III: It includes ten rats. They were be given atorvastatin in a dose of 40 ml\kg b.w orally through orogastric tube daily for 4 weeks and divided into two subgroups.

Group III a(animal model): sacrefied 24h after the last dose.

Group III b (recovery group): sacrefied 2weeks after the last dose.

Group IV : It includes ten rats. They were given atorvastatin in a dose of 40 ml\kg b.w orally through orogastric for 4 weeks followed by nanocurcumin in a dose of 15mg\kg b.w orally daily for 4weeks.

The animals were sacrificed at the end of experiment. 24h after the last dose, the animals were sacrificed. Specimens of skeletal muscles of (Gluteus, Biceps femoris, gastrocnemius) were obtained and fixed in formalin 10% for 24 hours. They were prepared for histological and immunohistochemical studies.

2.5 Methods

After 24 hours from the last dose, rats were anesthetized using ether inhalation, sacrificed, carefully dissected and specimens from skeletal muscles of (Gluteus, Biceps femoris, gastrocnemius) were processed for Haematoxyline and eosin and immunohistochemical stains.

2.6 Preparation of the Specimens for Light Microscopic Examination

Perfusion fixation was used and the specimens were fixed in 10% neutral buffered formalin and processed for light microscopic study. Paraffin sections of 6µm thickness were obtained for Hematoxylin and eosin and immunohistochemical stains**.** All histological technique was done according to **[13].**

2.7 Immunohistochemistry

2.7.1 Staining procedure

Tissue paraffin embedded 5µm thick sections were performed on coated glass slides. They were prepared for stanning with

- Active caspase -3 for detection of apoptotic cells
- CD117 for detection of satellite cells

The slides were de paraffinized in xylene and rehydrated using descending grades of alcohols (100%, 90%, 80% and 70%), then put in distilled water for 5 min. Endogenous peroxidase activity was blocked by immersion in 0.6% hydrogen peroxide for 10 minutes using peroxidase blocking reagent. Antigen retrieval was done by boiling slides in a microwave oven at a high temperature (80°C) for 10 min in citrate buffer solution (pH 6.0). The sections were incubated with the primary antibody at 4°C for 18–20h, washed in phosphate-buffered saline (pH7.2) and incubated with biotinylated secondary antibodies then with the avidin–biotin complex. All incubations were done at room temperature and the staining was visualized with diaminobenzidine and chromogen 25: 1. The sections were finally counterstained with haematoxylin, dehydrated, cleared, and mounted **.**The positive reaction appeared as brown coloration Negative control slides were done with omission of the 1ry antibodies using non-immunized goat sera.. Positive control slides for each antibody were used according to manufacturer instructions.

2.8 Morphometric Studies

Ten high power fields (x400) form each animal slide in all groups were photographed using

microscope Leica ICC50 Wetzlar (Germany). Analysis of each field was done using Image J software (version 1.46r) for measuring the percentage area of the immune reactive positive cells for active caspase-3 and CD117.

2.9 Statistical Analysis

All data were expressed as mean ± standard error (SEM). Data analyses were performed using SPSS software (version 16.00; SPSS Inc., Chicago, Illinois (|USA). Data analyses of different groups were performed using independent t -test, and Least Significant Difference (LSD) with a statistical significance of $P<0.05$. Graph were drawn in the Graph Pad Prism software (version 6).

3. RESULTS

Nanocurcumin particles was examined by the transmission electron microscope that showed the size of nanocurcumin, particles ranging from 24 nm up to 30 nm. (Fig.1)

Both group I& II showed the same histological findings. The longitudinal section (L.S) of the skeletal muscle fibers revealed that the muscle fibers appeared cylindrical multinucleated fibers .Elongated nuclei were found peripherally just under the sarcolemma. The sarcoplasm was acidophilic with longitudinal and transverse striations. (Fig.2)

In group IIIa, L.S of the skeletal muscle fibers showed disorganized, fragmented and discontinued muscle fibers. Splitting and hypertrophy of muscle fiber were frequently observed with loss of transverse and longitudinal striations of the myofibers. Cellular infiltration in perimysium was observed. The cytoplasm contained dense central nuclei, as well as remnants of necrotic nuclei Nuclear chain phenomena was also observed. Some nuclei were internal rather than peripheral to the muscle fibers. (Fig.3)

In group IIIb, L.S of skeletal muscle fibers revealed that there was apparent recovery of some myofiber in the form of restoration of the longitudinal striations no splitting, with peripheral nuclei. (Fig.4)

In group IV**,** L.S of skeletal muscle fibers appeared more or less as the control group. the transverse and longitudinal striations were restored .The nuclei were peripheral with minimal internal nuclei and cellular infiltration. (Fig.5).

3.1 Immunohistochemical Stanning

3.1.1 Active caspase-3

In both group I& II, examination of active caspase -3 stained sections of showed revealed negative immune reaction. Fig.6

In group IIIa, there was a marked increase in the number of active caspase -3 immune positive cells.Fig.7

In group IIIb, Examination of active caspase -3 stained sections revealed moderate increase in the number of active caspase -3 immune positive cells Fig.8

In group IV,examination of active caspase -3 stained sections) revealed minmal increase in the number of active caspase -3 immune positive cells. Fig.9.

3.1.2 CD117/C-KIT

Examination of CD 117 stained sections of the control groups (group I) and (group II) revealed positive immune reaction in satellite cell in endomysium. They were oval cells with long, slender processes there were located interstitial and peri fibrillar, adjacent to the sarcolemma of muscle fibers. Their distribution along the muscular fiber appeared to be random, with various positions. They either were oriented parallel or perpendicular to the longitudinal axis of the muscle fiber. Fig.10.

In group III a, examination of CD 117stained sections showed scanty staining positive satellite cells. Fig.11.

In group IIIb, examination of CD 117stained sections revealed increase in number of satellite cells staining positive cells . Fig.12.

In groupIV, examination of CD 117stained sections revealed increase in the number of stainning positive satellite cells. Fig.13.

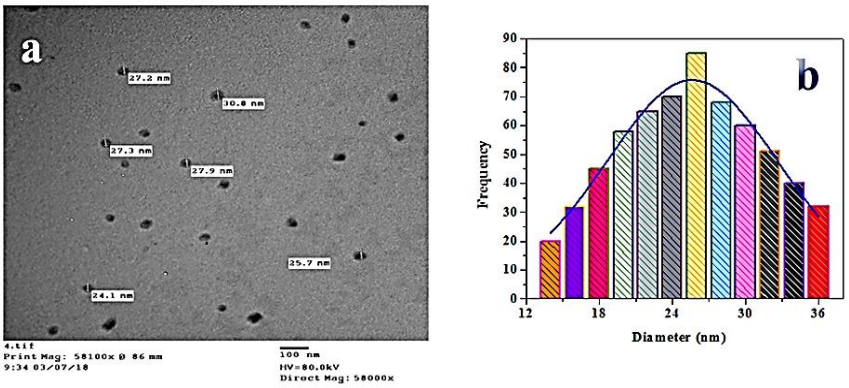

Fig.1. (a) TEM image of the prepared nano curcumin and (b) Histogram for particle size distribution of the prepared nano curcumin

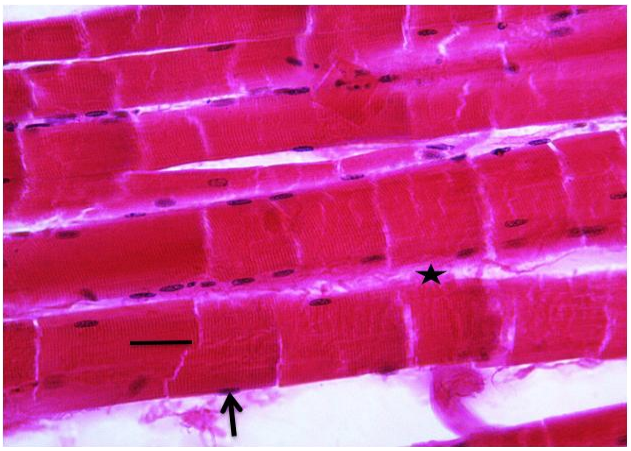

Fig. 2. A photomicrograph of a longitudinal section of skeletal muscles showing ., transverse and longitudinal striation of myofiber (line),the nuclei are located peripherally just beneath the sarcolemma (arrow)with minimal CT in between muscle bundles(star). Group I Hx&E X400)

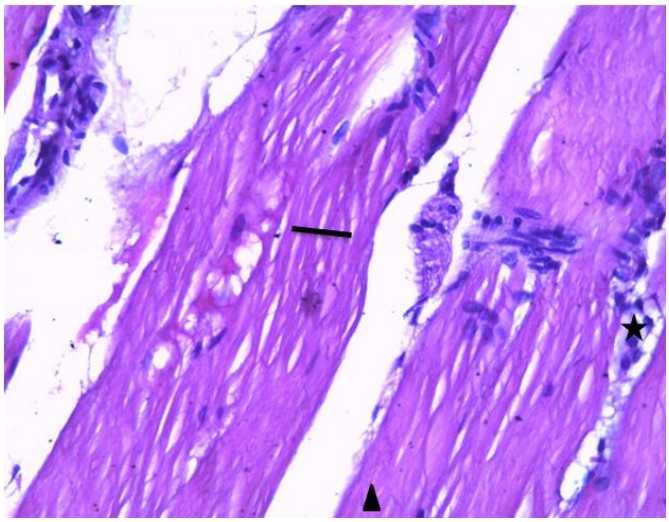

Fig. 3. A photomicrograph of a longitudinal section of skeletal muscles showing., splitting of myofibers (line), fragmentation of its sarcoplasm (arrowhead) and cellular infiltration in perimysium (star). (Group IIIa Hx&E X400)

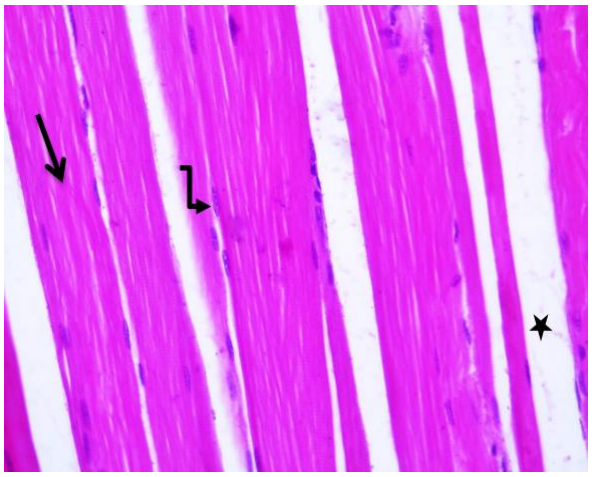

Fig. 4. A photomicrograph of a longitudinal section of skeletal muscles showing ., preserved longitudinal striations (straight arrow) ,minimal splitting, peripheral vesicular flat nuclei (curved arrow) with connective tissue in between muscle bundles (star). (Group IIIb Hx&E X400)

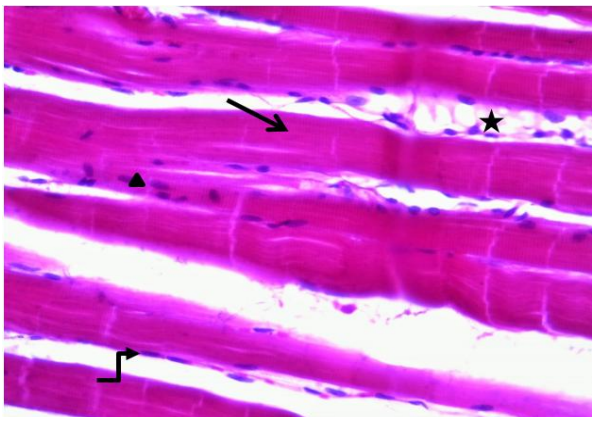

Fig. 5. A photomicrograph of a longitudinal section of skeletal muscles showing ., preserved transverse and longitudinal striations(straight arrow), peripheral nuclei (curved arrow) with minimal internal nuclei (head arrow)and minimal cellular infiltration (star) . (Group IV HX&E X400)

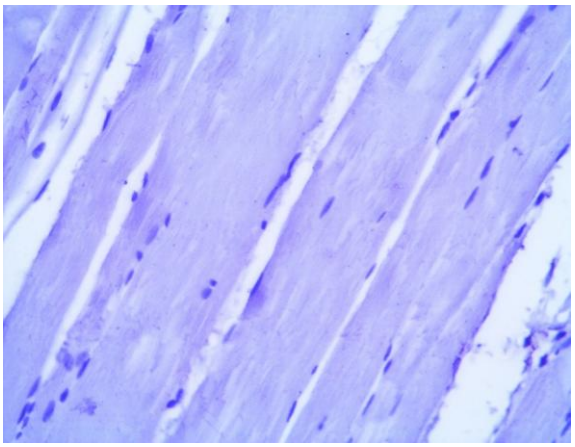

Fig. 6. A: photomicrograph of a longitudinal section of the skeletal muscles showing, no expression of active caspase-3 positive cells. (Group I active caspase-3 X400)

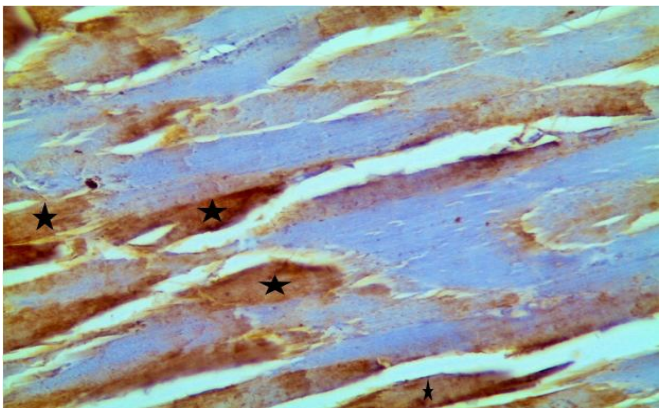

Fig. 7. A photomicrograph of a longitudinal section of the skeletal muscles showing., marked expression of active caspase-3 positive cells (stars)compared to group I &II. (Group IIIa active caspase-3 X400)

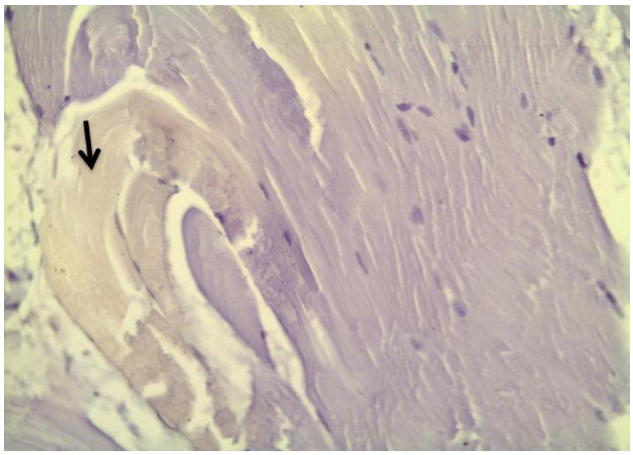

Fig. 8. A photomicrograph of a longitudinal section of the skeletal muscles showing., moderate expression of active caspase-3 positive cells(arrow) compared to group IIIa. (Group IIIb active caspase-3 X400)

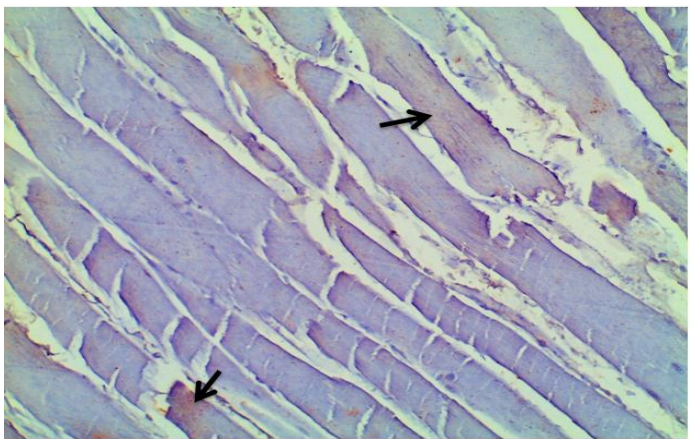

Fig. 9. A photomicrograph of immunohistochemical staining of skeletal muscles of group4 showing., minimal expression of active caspase-3 positive cells (arrow) compared to group IIIa. (GroupIV active caspase-3 X400)

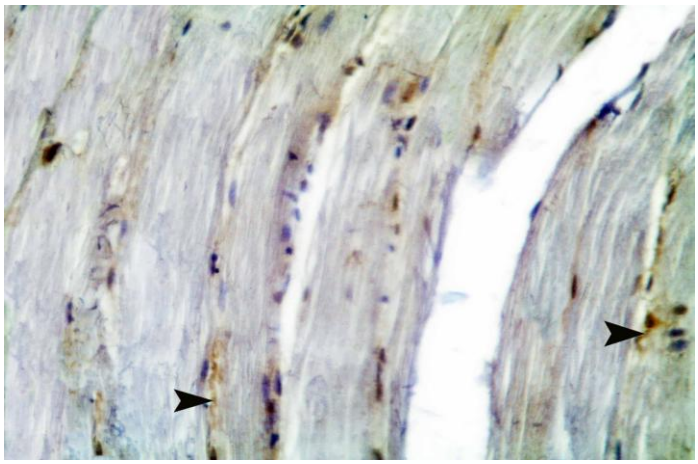

Fig. 10. A photomicrograph of immunohistochemical staining of skeletal muscles showing, scanty expression of CD117positive cells (arrow). (Group 1 CD117 X400)

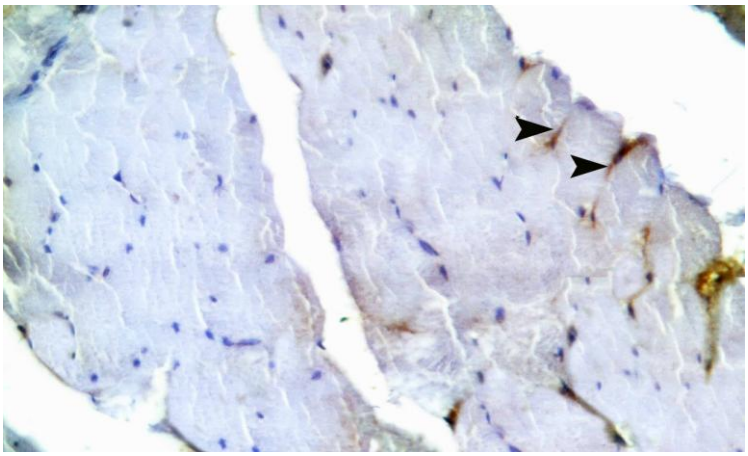

Fig. 11. A photomicrograph of immunohistochemical staining of skeletal muscles showing., scanty expression of CD117positive stalliete cells (arrow). (Group IIIa CD117 X400)

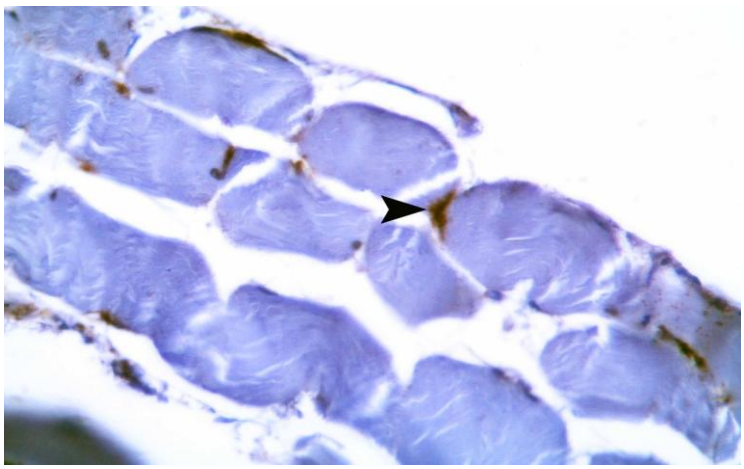

Fig.12. A photomicrograph of immunohistochemical staining of skeletal muscles showing., increased expression of CD117positive satellite cells (arrow). (GroupIIIb CD117 X400)

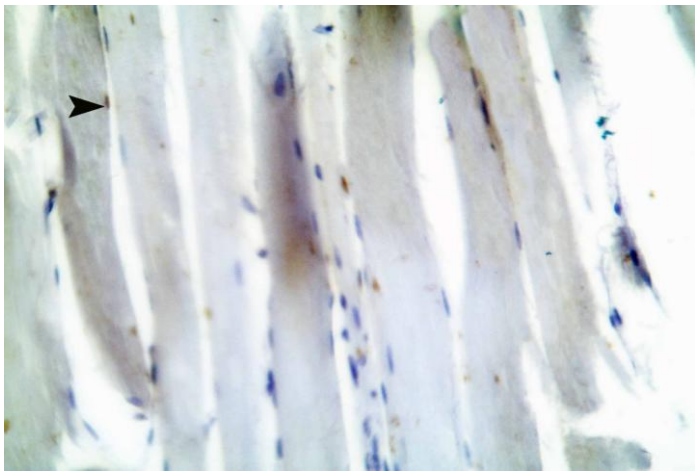

Fig. 13. A photomicrograph of immunohistochemical staining of skeletal muscles showing., increased expression of CD117positive satellite cells (arrow). (Group IV CD117 X400)

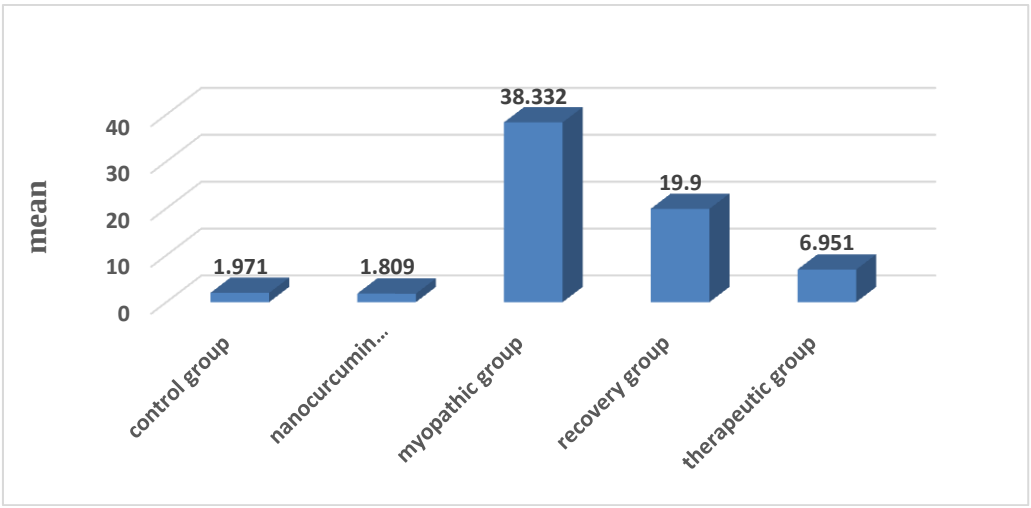

Histogram I. Mean measurement of area density of active caspase -3positive cells of control, nano curcumin control, myopathy, recovery and therapeutic groups

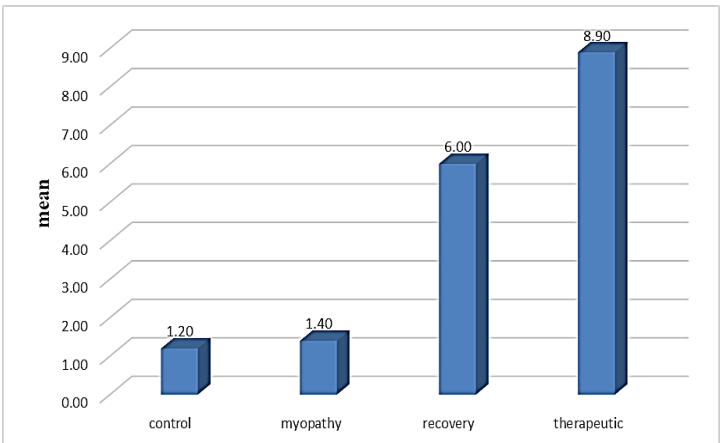

Histogram II. Mean measurement of CD 117 positive cells control, myopathy, recovery and therapeutic groups

4. DISCUSSION

The size of the prepared nano curcumin was confirmed by TEM analysis as shown in Figure 1 and the calculated histogram for particle size distribution shows that the mean particle size is confirmed nano sized particles of Curcumin is 26 nm [10,11,12].

Statins are reversible competitive inhibitors of 3-hydroxy-3-methylglutaryl-coenzymeA reductase (HMG CoA R) that reduce the intracellular synthesis of cholesterol [1]. Although statins could be tolerated, many degrees of myopathy ranging from mild myalgia to rhabdomyolysis have been reported.

This present work was done to show the potential myotoxicity of atorvastatin. We choose the vastus medialis of the quadriceps femoris and gastrocnemius muscle as they are formed mostly of type II white fibers which were reported by previous studies to be selectively vulnerable to statin‐induced myotoxicity [14,15].

Hematoxylin and eosin stain of myopathic group revealed focal areas of degenerative changes. They were manifested by splitting of the muscle fibers, fragmentation of the sarcoplasm, loss of transverse and longitudinal striations. Nuclear chain and dense centrally located nuclei were frequently observed. Furthermore, we found inflammatory cell infiltrations. These results were in agreement with literature [16,17].

Degeneration and inflammatory cellular infiltrations in the skeletal muscle fibers were noticed by many investigators using a variety of statins [18]. It was proved that splitting of the muscle fibers might be due to the insufficient oxygen supply as reported [19].

It could be suggested that the degenerative changes of the affected muscle fibers might be the stimulus that initiate the inflammatory reactions. This was in accordance with Stevnes and Lowe, 2000 who stated that the degenerated fibers release different inflammatory mediators that lead to mononuclear cellular infiltration [20].

In recovery group, some myofibers were noticed with linearly arranged euchromatic nuclei. Transverse and longitudinal striations start to be restored. These findings were in accordance with [21] who found that Patients with statin-associated myopathy experienced full resolution of muscle pain on cessation of statin therapy.

Caspases play a key role in apoptosis [22]. In this study, there was a high significant expression of active caspase 3-immuno positive reaction of the muscle fiber as compared to the control group. This was in agreement with the study of Mazroa and Asker,2010 who observed high expression of active caspase 9 in rat skeletal muscle after 10 mg/kg of atorvastatin treatment[17]. In agreement with our results Urso et al., 2005 proved that atorvastatin induced apoptosis in the skeletal muscle [23].

Different statins can induce apoptosis in the skeletal muscle. This result was explained by Rallidis et al., 2012 who found that statin induced myotoxicity through depletion of isoprenoids that control the rate of myofiber apoptosis. The depletion of isoprenoids are responsible for induction of apoptosis. Isoprenoids are also required for synthesis of ubiquinone which is a component of the electron transport chain. The reduction of isoprenoids associated proteins increases cytosolic calcium, which activates a cascade of events leading to the activation of caspase-3 [24].

In spite of the degenerative findings that encountered in the present study and in other studies, some researches considered atorvastatin and the other statins safe to use even in high doses [25] and consider statins the most effective prescribed drugs for lowering serum cholesterol [26].

Satellite cells are inactive, reserve myoblasts that persist after muscle differentiation. After injury or certain other stimuli, the normally quiescent satellite cells are activated, proliferate and fuse to form new skeletal muscle fibers [27].

In this study we found CD117 positive cells in satellite cell in endomysium. They were oval cells with long, slender processes they were located interstitial and peri fibrillar, adjacent to the sarcolemma of muscle fibers. Their distribution along the muscular fiber. In agreement with our suggestion Ceausu et al., 2016 found the same results in post mortum examination of skeletal muscles[28].

In contrary to our suggestion which consider a positive reaction for CD117/c-kit is suggestive for SCs, Popescu et al., 2011 suggested that stem cells from the muscle stem cell niche lack the immunopositivity for CD117, these positive CD117 cells being considered as telocytes [29].

In therapeutic group by using H&E, we found that some myofibers were noticed with vesicular peripherally arranged euchromatic nuclei with reappearance of transverse and longitudinal striations. These findings might indicate the presence of regenerating fibers that usually appeared near areas of necrosis and degeneration.

The current study showed that the use of nanocurcumin particles after atorvastatin ingestion led to a marked improvement of histopathological, immuno histochemical changes. Curcumin is an anti-inflammatory and an antioxidant agent which modulates the oxidative stress manifestations of atorvastatin in different types of muscles.

Curcumin had inhibitory actions in tissue injury mediated by the inflammatory transcription factors, protein kinases, oxidative stress, and inflammation [4].

Manjunatha and Srinivasan, 2007 reported that curcumin has an antioxidant effect based on lipid peroxidation modulation and the increase of antioxidant enzyme activity because it reverses glutathione depletion which is consistent with our results [30].

In agreement with our results Pinlaor et al., 2010 had reported that curcumin increased the serum matrix metalloproteinases MMP-13 levels that are responsible for the restoration of normal collagen distribution in the muscle fibers [31].

5. CONCLUSION

Atorvastatin caused histopathological changes of the skeletal muscles through induction stress and apoptotic changes while nanocurcumin particles have anti-oxidant effects and led to marked improvement of these histopathological changes. Recovery of some histopathological changes after stoppage of atorvastatin treatment.

6. RECOMMENDATION

Further studies should be done in animals using nano curcumin as a protective agent, also using ordinary curcumin instead of nano curcumin. Extra studies should be done in human with different concentrations.

CONSENT

It is not applicable.

ETHICAL APPROVAL

The Institutional Animal Care and the Research Ethics Committee of the Faculty of Medicine, Sohag University, Egypt, approved the experimental protocol.

COMPETING INTERESTS

Authors have declared that no competing interests exist.

REFERENCES

1. Schachter M. Chemical, pharmacokinetic and pharmacodynamic properties of statins: an update. Fundamental & Clinical Pharmacology. 2005;19:117–125.
2. Marcoff L, Thompson PD. The role of coenzyme Q10 in statin-associated myopathy: a systematic review. Journal of the American College of Cardiology. 2007;49(23):2231-2237.
3. Panahi Y, Hosseini MS, Khalili N, Naimi E, Simental-Mendía LE, Majeed M, Sahebkar A. Effects of curcumin on serum cytokine concentrations in subjects with metabolic syndrome: A post-hoc analysis of a randomized controlled trial. Biomedicine & Pharmacotherapy. 2016;82: 578-582.
4. Aggarwal BB, Harikumar KB. Potential therapeutic effects of curcumin, the anti-inflammatory agent, against neurodegenerative, cardiovascular, pulmonary, metabolic, autoimmune and neoplastic diseases. The International Journal of Biochemistry & Cell Biology. 2009;41(1):40-59.
5. Popescu LM, Manole E, Şerboiu CS, Manole CG, Suciu LC, Gherghiceanu M, Popescu BO. Identification of telocytes in skeletal muscle interstitium: implication for muscle regeneration. Journal of Cellular and Molecular Medicine. 2011;15(6): 1379-1392.
6. Manjunatha H, Srinivasan K. Hypolipidemicand antioxidant effects of curcumin and capsaician in high-fat-fed rats. Canadian Journal of Physiology andPharmacology. 2007;85:588–596
7. Allegri P, Mastromarino A, Neri P. Management of chronic anterior uveitis relapses: efficacy of oral phospholipidic curcumin treatment. Long-term follow-up. Clinical Ophthalmology (Auckland, NZ). 2010;4:1201.

8. Anand P, Kunnumakkara AB, Newman RA, Aggarwal, BB. Bioavailability of curcumin: problems and promises. Molecular Pharmaceutics. 2007;4(6):807-818.
9. Gupta SC, Patchva S, Aggarwal BB. Therapeutic roles of curcumin: lessons learned from clinical trials. The AAPS Journal. 2013;15(1):195-218.
10. Abdel-Rahman LH, Abu-Dief AM, El-Khatib RM, Abdel- Fatah SM. Sonochemical synthesis, DNA binding, antimicrobial evaluation and in vitro anticancer activity of three new nano-sized Cu(II), Co(II) and Ni(II) chelates based on tridentate NOO imine ligands as precursors for metal oxides. J. Photochem. Photobio. B 2016;162:298–308.
11. Adel A, Marzouk, Ahmed M, Abu-Dief, Antar A, Abdelhamid. Hydrothermal preparation and characterization of $ZnFe_2O_4$ magnetic nanoparticles as an efficient heterogeneous catalyst for the synthesis of multi-substituted imidazoles and study of their anti-inflammatory activity, Appl Organometal Chem. 2018;32(1):e3794.
12. Sameerah I, Al-Saeedi, Laila H, Abdel-Rahman, Ahmed M, Abu-Dief, Shimaa M, Abdel-Fatah, Tawfiq M. Alotaibi, Ali M. Alsalme and Ayman Nafady, Catalytic Oxidation of Benzyl Alcohol Using Nanosized Cu/Ni Schiff-Base Complexes and Their Metal Oxide Nanoparticles, Catalysts. 2018;8(452):1-14.
13. Bancroft JD. Histochemical techniques. Butterworth-Heinemann; 2013.
14. Hanai H, Sugimoto K. Curcumin has bright prospects for the treatment of inflammatory bowel disease. Current Pharmaceutical Design. 2009;15(18):2087-2094.
15. Westwood FR, Bigley A, Randall K, Marsden AM, Scott RC. Statin induced muscle necrosis in the rat: Distribution, development and fibre selectivity. Toxicol Pathol. 2005;33:246-257
16. Khalil MS, Khamis N, Al-Drees A, Abdulghani HM. Does coenzyme-Q have a protective effect against atorvastatin induced myopathy? A histopathological and immunohistochemical study in albino rats. Histol Histopathol. 2015;30(3):383-90
17. Mazroa SA, Asker SA () Myotoxic Effects of Atorvastatin Drug (Lipitor) on the Skeletal Muscles of Adult Male Albino Rats and the Effect of L-Carnitine Co-administration Light Microscopical, Immunohistochemical and Biochemical Study. Egypt. J Histol. 2010;33:520- 531
18. Pierno S, Didonna MP, Cippone V, De Luca A, Pisoni M, et al. Effects of chronic treatment with statins and fenofibrate on rat skeletal muscle: a biochemical, histological and electrophysiological study. Br J Pharmacol. 2006;149:909-919.
19. Hassan NF, El-Bakry NA, Shalaby NM, Ghobara MM, Bayomi NA. Histological Study of the Effect of Simvastatin on the Skeletal Muscle Fiber in Albino Rat and the Possible Protective Effect of Coenzyme Q 10. Egypt. Histol. 2009;31:216-226.
20. Stevnes A, Lowe J. Tissue response to damage. In: Stevnes A, Lowe J,edtr. Pathology. (2nd ed.) Mosby. 2000:35-60.
21. Hansen KE, Hildebrand JP, Ferguson EE, Stein JH. Outcomes in 45 patients with statin-associated myopathy. Archives of Internal Medicine, 2005;165(22):2671-2676.
22. Shi Y. Caspase activation: revisiting the induced proximity model. Cell. 2004;117: 855-858.
23. Urso ML, Clarkson PM, Hittel D, Hoffman EP, Thompson PD. Changes inubiquitin proteasome pathway gene expression in skeletal muscle with exercise and statins. Arterioscler Thromb Vasc Biol. 2005;25:2560-2566.
24. Rallidis LS, Fountoulaki K, Anastasiou-Nana M. Managing the underestimated risk of statin-associated myopathy. International journal of cardiology. 2012;159(3):169-176.
25. Shibata M, Hattori H, Sasaki T, Gotoh J, Hamada J, Fukuuchi Y. (). Activation of caspase-12 by endoplasmic reticulum stress induced by transient middle cerebral artery occlusion in mice. Neuroscience. 2003;118(2):491-499.
26. Sun XM, MacFarlane M, Zhuang J, Wolf BB, Green DR, Cohen GM. Distinct caspase cascades are initiated in receptor-mediated and chemical-induced apoptosis. Journal of Biological Chemistry. 1999;274(8):5053-5060.
27. Yin H, Price F, Rudnicki MA. Satellite cells and the muscle stem cell niche. Physiological Reviews. 2013;93(1):23-67
28. Ceausu M, Hostiuc S, Dermengiu D. Skeletal muscle satellite stem cells at different postmortem intervals. Rom J Leg Med. 2016;24:23-27
29. Popescu LM, Manole E, Şerboiu CS, Manole CG, Suciu LC, Gherghiceanu M,

Popescu BO. Identification of telocytes in skeletal muscle interstitium: implication for muscle regeneration. Journal of Cellular and Molecular Medicine. 2011;15(6): 1379-1392.

30. Manjunatha H, Srinivasan K. Hypolipidemicand antioxidant effects of curcumin and capsaician in high-fat-fed rats. Canadian Journal of Physiology andPharmacology. 2007;85:588–596

31. Pinlaor S, Prakobwong S, Hiraku Y, et al. Reduction of periductal fibrosis in liver flukeinfected hamsters after long-term curcumin treatment.European Journal of Pharmacology. 2010;638: 134–141.

Peer-review history:
The peer review history for this paper can be accessed here:
https://www.sdiarticle5.com/review-history/81351